Nikam and Patil *J Wireless Com Network* (2023) 2023:104
https://doi.org/10.1186/s13638-023-02306-8

EURASIP Journal on Wireless Communications and Networking

RESEARCH

Open Access

Design and development of multiband PIFA antenna for vehicular LTE/5G and V2X communication

Amruta A. Nikam[1*] and Rupali B. Patil[1]

*Correspondence: amrutanikam511@gmail.com

[1] Department of Electronics and Telecommunication Engineering, G. H. Raisoni College of Engineering and Management, Pune 412207, India

Abstract

This paper aims to introduce a custom-designed multiband planar inverted-F antenna (PIFA) suitable for automotive applications in LTE/5G schemes operating under 6 GHz, as well as Vehicle-to-Everything (V2X) communications. The PIFA antenna has a broad bandwidth capability, resonating from 950 MHz to 6 GHz. The proposed PIFA antenna is divided into three parts: the top, front, and back, resulting in a unique and effective antenna structure. The antenna is fabricated using a substrate made of FR4 material with a dielectric constant of 4.4. The whole measurements of the antenna are $54 \times 38 \times 25$ mm^3.The proposed PIFA antenna has been tested and has achieved a voltage standing wave ratio (VSWR) of less than 2 across the entire frequency range of 950 MHz to 6 GHz. Additionally, the maximum gain achieved by the antenna is 7.08 dBi at a frequency of 5.5 GHz, 6.81 dBi at 5.2 GHz, and 6.65 dBi at 5.9 GHz. The antenna also achieved a gain of 6.67 dBi at 3.8 GHz and a gain of 3.31 dBi at 1.7 GHz. Overall, this paper presents a well-designed and effective multiband PIFA antenna that is appropriate for use in vehicular applications. The antenna ability to cover a wide range of bandwidth and achieve high gain makes it an excellent candidate for use in LTE/5G systems and V2X communications.

Keywords: PIFA, Multiband, V2X communications, LTE/5G

1 Introduction

With the development of 5G and V2X communications during the earlier 20 years, the integration of sensors and wireless technologies has dramatically changed the locomotive sector. These technologies are essential for the development of driverless vehicles as well as for boosting driving enjoyment and road safety. Severe socioeconomic issues including longer travel times and auto accidents are a result of town traffic jamming. In order to maximize traffic safety, enhance the self-driving experience, and connect to the Internet of Things (IoT), vehicles can communicate with each other, people, and infrastructure. With the cellular network serving as a backup for short-range communication and offering internet access outside of DSRC range, 5G networks and DSRC can cooperate to deliver V2X communication solutions [1].

The dedicated short-range communications (DSRC) network is a wireless communication system designed to provide short-range communication between vehicles and infrastructure. In the USA, the Federal Communication Commission (FCC) has assigned the frequency band between 5.850 and 5.925 GHz forV2X Communication.

The Department of Transportation (DOT) has specified the use of DSRC technology for vehicle-to-vehicle (V2V) and vehicle-to-infrastructure (V2I) communication to enhance transportation safety, reduce congestion, and improve mobility. DSRC technology permits vehicles to talk with nearby vehicles and roadside infrastructure, including traffic signals, signs, and other roadside equipment.V2X is being used in numerous uses like collision avoidance, detection, intersection safety, and emergency vehicle warning systems. It is also being used in public transportation systems to advance the competence and protection of bus and rail operations.

However, in December 2020, the FCC voted to reallocate a portion of the DSRC spectrum for unlicensed use by Wi-Fi devices. This decision has been controversial, as it may impact the reliability and effectiveness of DSRC for transportation safety and mobility applications. The DOT has been evaluating alternative spectrum options for DSRC and exploring new technologies like cellular vehicle-to-everything (C-V2X) as potential alternatives [2, 3].

The development of antennas for vehicles is a difficult task due to several factors, including size limitations, coupling between different elements, and the need to accommodate multiple applications within a restricted-size package. Modern vehicles often require antennas for various applications such as cellular communication, GPS navigation and traditional AM/FM radio.

To address these challenges, antenna designers often use advanced techniques such as multiband and wideband antennas, antenna diversity, and electromagnetic shielding. Multiband antennas are capable of covering multiple frequency bands, reducing the need for separate antennas. Wideband antennas can operate over a broad range of frequencies, allowing them to accommodate multiple applications within a single antenna. Antenna diversity techniques involve using multiple antennas to improve signal quality and reduce interference [4, 5].

Furthermore, designers can also use electromagnetic shielding to isolate different antenna elements from each other, reducing coupling and interference. Designing antennas for vehicles is a complicated process that involves taking into account various factors to ensure that communication systems are dependable and efficient, while also meeting size limitations. As a result, fitting multiple antennas into a restricted space can be a challenging task [6, 7].

With the advent of 5G and DSRC technologies, there is a need for multiband antennas that can cover a wide frequency range with reasonable physical dimensions. In this article, we suggest a multiband PIFA antenna that can work over the frequency bands from 950 MHz to 6 GHz for automotive applications. Compared to existing works in literature, the proposed antenna achieves a wider frequency bandwidth with reasonable physical dimensions.

Although [8] presents a compressed 3D antenna that worked from 790 MHz to 2.69 GHz, it falls short in covering the required bandwidth for 5G, which ranges from 617 MHz to 5 GHz. Furthermore, the antenna designs presented in [9, 10] have larger dimensions than the planned design and do not completely shelter the preferred frequency band. Additionally, the antenna designs in [11–16] cover less frequency bandwidth than the planned design while also having an advanced physical height. The planned antenna design in this paper comprises a radiating patch with a wine glass-shaped slot, as well as a ground plane with a switchable rectangular ring-type slot.

This antenna is capable of achieving multiband resonances by including slots in both the key radiating component and the ground plane. In order to switch between the various resonant frequencies, the antenna design incorporates two PIN diodes that are strategically placed on the four-sided ring slot in the ground level. These PIN diodes are able to change the electrical characteristics of the antenna by either opening or closing the switchable slot. This effectively allows the antenna to operate at different frequencies depending on the state of the PIN diodes [17].

The antenna design presented in this paper operates at high frequencies by incorporating two branches, and for wider bandwidth, these branches are added as a tapered structure to improve impedance matching. The antenna covers a wide frequency range of 824–960 MHz, 1710–2690 MHz, and 3.4–3.6 GHz, making it suitable for use in GSM, LTE, and 5G systems. The maximum gain achieved by the antenna is 3.54 dBi at 900 MHz, 5.89 dBi at 2100 MHz, and 3.52 dBi at 3.5 GHz [18].

The fractal monopole configuration with defected ground structure exhibits a multiband performance at frequencies of − 2.4 GHz, 5.1 GHz, and 5.95 GHz, with a gain of − 3.4 dB at 2.4 GHz, a fractional bandwidth of 35.05%, and a radiation efficiency of 80% [19]. The planned multiband antenna is planned to shield a wide range of frequencies, comprising 5G sub-6 GHz and LTE bands oscillating from 617 to 5000 MHz, the advanced GNSS band from 1559 to 1606 MHz, and the V2X band at 5.9 GHz [20]. The self-affine fractal construction offers versatility in the design of tiny antennas. By choosing the right scaling factor and optimizing the feed position, the harmonic gasket antenna displays multiband resonance [21–23].

When it comes to designing multiband antennas for vehicle communication, covering a wide frequency band with a single antenna can be a challenging task. However, the planar inverted-F antenna (PIFA) structure has proven to be an effective solution for achieving this goal while maintaining a low profile. PIFA antennas are designed to resonate over a wide frequency band and can be easily integrated into a variety of applications, including vehicle communication systems. By using a PIFA structure, it is possible to cover multiple frequency bands with a single antenna, thereby simplifying the overall system design and reducing the complete size and weight of the antenna. Moreover, PIFA antennas have a low profile and are well-suited for use in applications where space is at a premium, such as in vehicle communication systems. These antennas can be designed to operate over a wide frequency band, making them an ideal choice for use in modern communication systems that rely on multiple frequency bands.

The design, manufacture, simulation, and measured outcomes of a PIFA antenna are all thoroughly examined in this research. To accomplish the necessary antenna characteristics, the design procedure comprises using HFSS software and combining mathematical computations. The antenna is then constructed using FR4 material and tested using a network analyzer. When compared to currently used antennas in the field, the performance of the proposed PIFA antenna performs better. The outcomes of the simulations and measurements offer insightful information on the PIFA antenna's effectiveness and efficiency. The thorough analysis and experimental validation provided in this study increase knowledge of and make use of antenna technology.

Overall, the PIFA structure is a proven solution for achieving wideband coverage with a low profile antenna. Its suitability for use in vehicle communication systems and other space-constrained applications makes it an attractive choice for modern communication systems. This paper concentrates on multiband resonance of antenna at targeted frequencies. The article is structured into the subsequent sections.

Section 2: Method

This section describes the design guidelines for the proposed antenna and presents the proposed antenna geometry. The antenna is designed using FR4 substrate with a thickness of 1.6 mm and a dielectric constant of 4.4. The proposed antenna geometry consists of 3 patch with one short arm.

Simulation and Dimension Tools:

To confirm the performance of the planned antenna design, it was simulated using HFSS software. The simulation results were then confirmed through experimental measurements using a vector network analyzer (VNA).

Section 3: Experimental work

This section presents the simulation and measurement results of the proposed antenna and compares it to existing designs in literature. The proposed antenna achieves a wider frequency bandwidth from 950 MHz to 6 GHz with rational physical proportions. Compared to existing designs, the proposed antenna outperforms in terms of frequency bandwidth and physical dimensions.

Section 4: Results Discussion

Section 5: Conclusion

This paper has described the design and development of a multiband PIFA antenna for use in automotive applications operating in the 5G and V2X frequency bands. The proposed antenna achieves a wider frequency bandwidth ranging from 1 to 6 GHz with compact physical dimensions, outperforming existing designs reported in the literature. Further work will involve optimization of the antenna design for enhanced performance and seamless integration into automotive systems.

2 Method

The suggested antenna comprises of a PIFA structure made from three rectangular patch antennas and copper foil. The substrate utilized is FR4, which has a loss tangent of 0.02 and a dielectric constant of 4.4. Due to its affordable price, wide availability, and lightweight characteristics, FR4 was chosen. The antenna was developed and optimized using Ansys HFSS software.

2.1 Design process

The planned antenna in this article is designed using a PIFA structure, which includes specific physical measurements and slots to enhance its low band working frequency and rise bandwidth, all while maintaining a smaller volume than previously reported designs. The antenna is constructed using a metal sheet of proportions of

Table 1 Proposed antenna design parameters

Parameter	L	W	H	S_g	S_l	H_{cut1}	H_{cut2}	F_l	F_h	W_s
Value (mm)	54	38	24	2.5	45	10	17	3	2	3

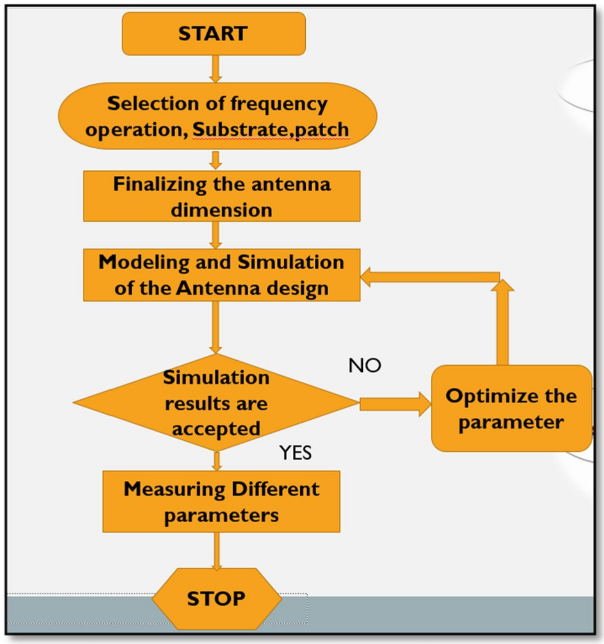

Fig. 1 Process flow of antenna design based on frequency of operation, substrate material used to fabricate antenna and selection of patch. The phases elaborated in creating an antenna based on frequency, substrate, and patch selection are potted in the figure. The first step in the technique is to select the operating frequency band. Next, the right substrate material is designated based on its dielectric constant, loss tangent, thickness, and price. The intended resonance frequency and radiation pattern are used to regulate the patch's size and shape. In the end, electromagnetic simulation software is used to simulate and enhance the antenna design before construction and testing

$54 \times 38 \times 25\ \text{mm}^3$ and is fixed on PCB which is act as ground. The gap among the three plates is filled with free space (air).

It stands critical for the mid and high bands to yield pleated monopole assemblies with slits that the wide feeding arm, as shown in b, be situated at the border of the horizontal plane. To regulate the resonance frequency of the low band, a short arm is likewise positioned at a certain space W after the feeding arm as illustrated in figure c. The optimized values for the antenna's various geometrical characteristics are shown in Table 1. The proposed design introduces two resonance frequencies in the medium- and high-frequency bands by adding three new structures with slots 1 and 2, as well as four additional incisions at the top. The designed process of antenna is shown in Fig. 1.

Main, in calculation to the shorting and feeding arm, the element's physical size define the low frequency band. Equations (1) through (3) are utilized in the design of an antenna's fundamental structure [24].

$$\text{Width}(w) = \frac{c}{2f_0\sqrt{(\text{sr}+1)/2}},\ E_{\text{eff}} = \frac{\text{sr}+1}{2} + \frac{\text{sr}+1}{2}\left[\frac{1}{\sqrt{1+12\left(\frac{h}{w}\right)}}\right] [24] \quad (1)$$

$$\text{Length(L)} = \frac{c}{2f_0\sqrt{s_{\text{eff}}}} - 0.842h\left(\frac{(s_{\text{eff}}+0.3)\left(\frac{w}{h}+0.264\right)}{(s_{\text{eff}}-0.258)\left(\frac{w}{h}+0.8\right)}\right) [24] \quad (2)$$

$$\text{Width of Short Arm } (Ws) = Ws \leq (0.05 - 0.1)\lambda \ [24] \quad (3)$$

The variables in the equation are defined as follows: c represents the speed of light which is equal to the product of the wavelength (λ) and frequency (f), h is the height of the substrate, W, L, and H are the width, length, and height of antenna, respectively. F_l and F_h represent the length and width of the antenna feed, W_s is the breadth of the shorting arm; S_l and S_g are length and width of slots in the top view, respectively, as illustrated in Fig. 2a–c.

The phases elaborated in creating an antenna based on frequency, substrate, and patch selection are potted in the figure. The first step in the technique is to select the operating frequency band. Next, the right substrate material is designated based on its dielectric constant, loss tangent, thickness, and price. The intended resonance frequency and radiation pattern are used to regulate the patch's size and shape. In

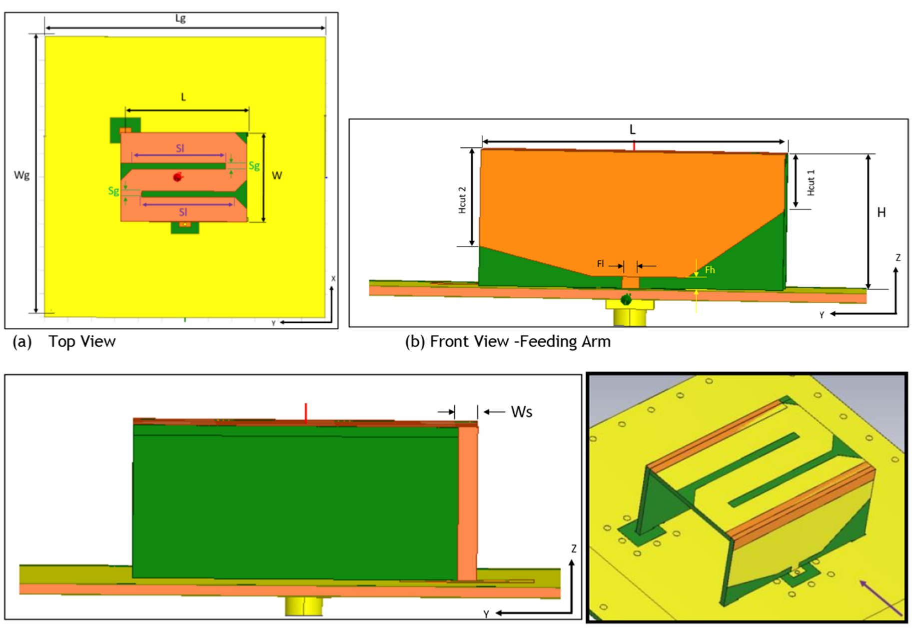

Fig. 2 Geometry of PIFA antenna. At the top of antenna two cuts are made of size 45 mm × 2.5 mm. Top view shorted to ground through short- arm as shown in **c**. Complete Integration of **a**, **b**, **c** results into final geometry of antenna. **a**, **b**, **c** Signify the top, front and back view of the proposed antenna. Overall, this figure provides a visual representation of the design of a PIFA antenna that could be used for wireless communication applications

the end, electromagnetic simulation software is used to simulate and enhance the antenna design before construction and testing.

The top view as shown in Fig. 2a of the antenna includes two slots measuring 45 × 25 mm, which helps to escalation the electrical distance of the antenna while sustaining a small antenna size. This results in a properly resonating antenna in higher frequency bands, similar to a patch antenna with a radiating distance of 54 mm and a width of 38 mm. The bandwidth of the mid frequency band, operating within the 1–3.5 GHz range, is determined by the width of slot 1. The top plate is directly connected to ground through a shorting arm which allows the antenna to resonate at desired frequency. Additionally, four extra cuts are made in the top plate to enhance the overall bandwidth of the antenna [25].

Figure 2b displays the front view of antenna (the feeding arm), two side cuts are visible, which aid in resonating the antenna in the high frequency group. The significance of the feeding arm with two side cuts in a PIFA antenna lies in its ability to modify the current distribution and reduce the influence of the ground plane on the antenna's impedance. This modification results in better impedance matching and higher efficiency. Furthermore, the side cuts can make the PIFA less susceptible to changes in the orientation of the device, providing more stable and consistent performance across different positions and angles.

In Fig. 2c which displays the back view of antenna (short arm), the frequency in middle band is controlled. The shorting arm in a PIFA antenna is significant because it enables the control of the antenna's resonance frequency. By adjusting the position and length of the shorting arm, the antenna's resonant frequency can be tuned to match the operating frequency requirements. Furthermore, the shorting arm helps in decreasing the size of the antenna by introducing a capacitive coupling among the top view and the ground plane, resulting in a shorter electrical length of the antenna. This reduction in size makes the PIFA antenna an ideal choice for wireless devices with limited space for antenna placement. In conclusion, the shorting arm is a crucial element that shows a noteworthy role in the size and performance of the PIFA.

3 Experimental work

To construct the planned antenna, the dimensions specified in Table 1 were taken into consideration. The fabricated prototype of the PIFA is shown in the accompanying Figs. 3, 4. The antenna is made-up using a FR4 substrate with a wideness of 1.6 mm. All three parts of the antenna, namely the top, front, and back, were joined together at the edges using copper foil. It is worth noting that this joining process may introduce some minute changes in the antenna's performance characteristics. To mount the complete assembly, a printed circuit board (PCB) measuring 120 × 120 mm was used as the ground plane. This allowed for the effective integration of the antenna into a larger communication system, such as a vehicle communication system. Overall, the use of a FR4 substrate and copper foil for joining the various antenna parts together, along with the incorporation of a PCB as the ground plane, were key design choices that contributed to the successful fabrication of the proposed PIFA antenna. The PIFA structure was put together by soldering the separate pieces.

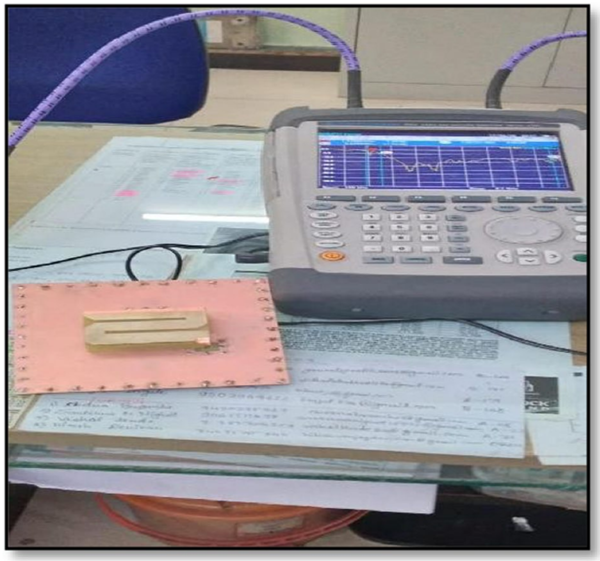

Fig. 3 Experimental set-up to test the antenna. The figure shows a network analyzer being used to test an antenna. A network analyzer is a specialized instrument used to measure the performance of electronic networks, including antennas. The network analyzer is connected to the antenna through a coaxial cable, which is used to transmit and receive signals

4 Results and discussion

The graph in Fig. 5 shows that there is a minor dissimilarity among the measured and simulated results for the s11 parameter, which could be due to the manual assembly of the antenna. The small variations can be attributed to manufacturing errors, such as tolerance in the soldering and SMA connectors, that were not accounted for in the simulations. The measured data were collected using network analyzer. The planned antenna is intended to resonate at frequencies ranging from 1.15 to 6 GHz, achieved by shorting the upper patch to the ground through a shorting arm. The maximum value of S11 (−29.13 dB) is obtained at 2.18 GHz, while at other frequencies, such as 3.5 GHz, 5.5 GHz, and 5.9 GHz, the s11 parameter is −15.62 dB, −13.75 dB, and −13.08 dB, respectively. The width of the feeding arm, W, can have a small effect on the resonance frequency in the lower band. Aggregating the breadth of the shorting arm will tune the antenna to a higher frequency. This is because the width of the feeding arm determines the amount of capacitance between the two arms, and changing this capacitance will alter the resonance frequency. Therefore, by increasing the breadth of the shorting arm, the overall capacitance of the antenna is decreased, resulting in a higher resonance frequency.

As shown in Fig. 6, the simulated VSWR of the antenna was related to the dignified VSWR, and it was observed that the measured VSWR was below 2 (approximately −10 dB return loss) through the working bands of 5G and V2X. To achieve good VSWR in the high-frequency band, the dimensions of slot 1 and slot 2 are crucial, and changing their length and width will have the most significant impact. This is because the slots' dimensions determine the amount of coupling between the two arms of the antenna, which affects the VSWR. Altering the slot dimensions can

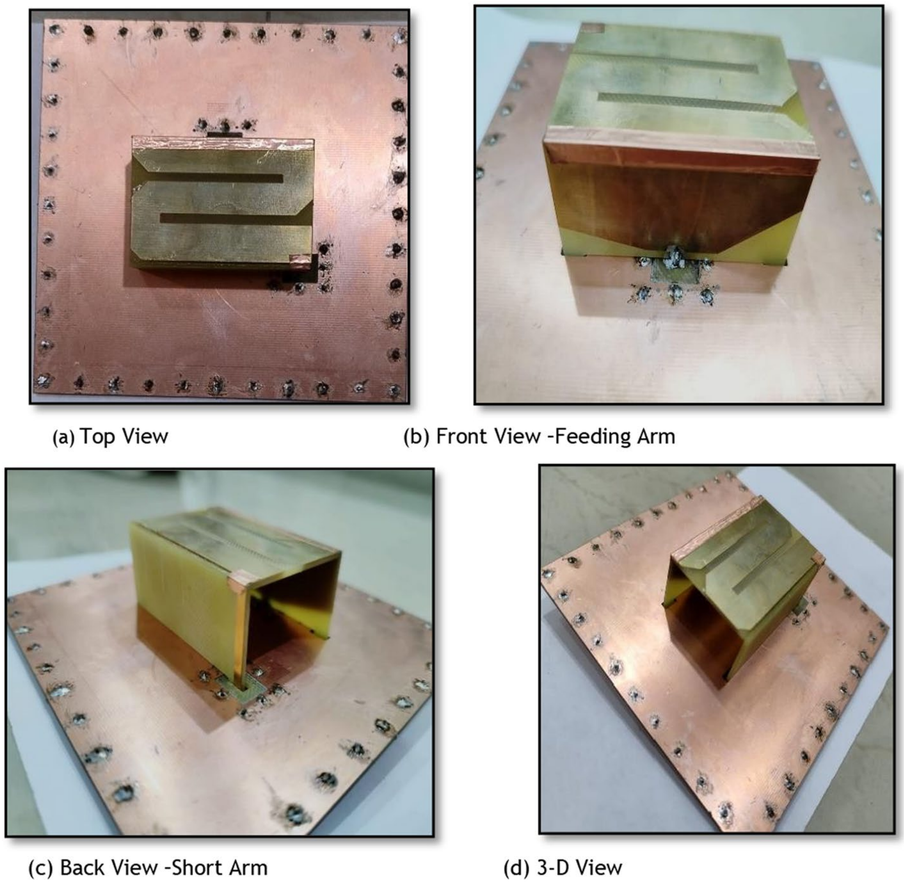

Fig. 4 The photographs of fabricated antenna. The photograph shows the PIFA antenna mounted on a substrate board, which is likely made of a dielectric material, such as FR-4. The PIFA is rectangular in shape and is placed at the center of the board. The antenna has a feed arm located at one end, which is connected to the feeding element that extends vertically from the patch to the ground plane. Top view is shown in **a** with two slots, Front view is shown in **b**, back view in **c**, 3-D view in **d**

change the coupling and therefore impact the VSWR. It is essential to optimize the slot dimensions to achieve the desired VSWR across all operating frequencies.

The simulated result of max. realized gain over Freq and for Theta 0°, 60° and 90° is depicted in Fig. 7. The maximum realized gain of the antenna concluded a range of frequencies from 1 to 6 GHz was found to be between − 0.2 and 7 dBi. The realized gain varies with the operating frequency and the angle of radiation. At a frequency of 1 GHz, the realized gain was approximately − 0.2 dBi, indicating that the antenna was not very efficient at converting input power into radiated power. However, as the frequency increased, the realized gain also increased, reaching a maximum of 7 dBi at some frequencies. The angle of radiation also affects the realized gain. At an angle of 0° (i.e., broadside radiation), the realized gain was generally higher than at other angles. For example, at 0°, the realized gain was approximately 5dBi at a frequency of 3.5 GHz, whereas at an angle of 60°, the realized gain was approximately 0 dBi. At an angle of 90° (i.e., endfire radiation), the realized gain was generally lower than at other angles. Overall, the antenna demonstrated good performance over the operating

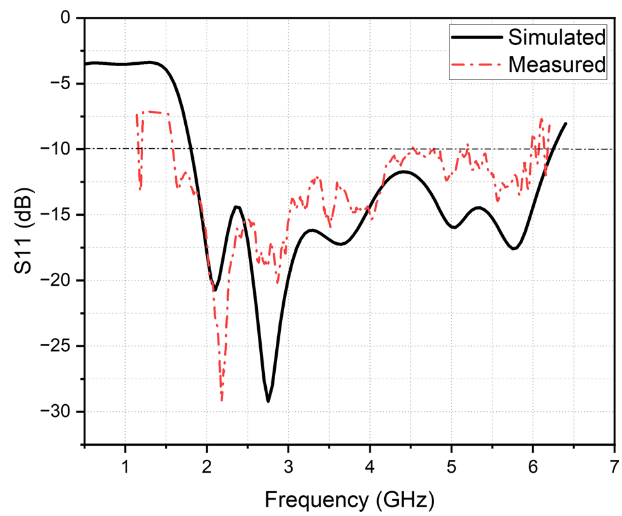

Fig. 5 Return loss was measured and modeled (S11). This graph shows the contrast between actual results and results from simulations. In comparison with the simulated outcomes, the measured results are slightly biased. The manual construction of the antenna could be to blame for the movement. The differences between the measured and the observed Small production mistakes are blamed for simulated results

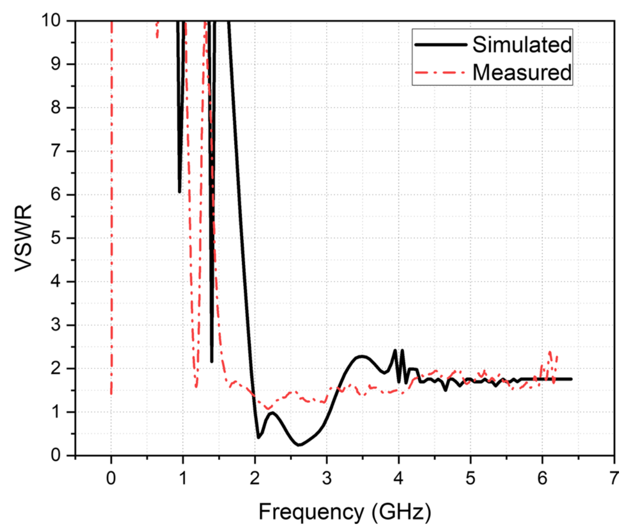

Fig. 6 VSWR was measured and modeled. This graph shows the contrast between actual results and results from simulations. In comparison with the simulated outcomes, the measured results are slightly biased. The manual construction of the antenna could be to blame for the movement. The differences between the measured and the observed Small production mistakes are blamed for simulated results. The SMA connectors, soldering, grounding, and patches on substrate as an industrial forbearance are examples of elements that were not included in simulations and are responsible for the small changes that are perceived

frequency range of 1–6 GHz, with a maximum realized gain of 7 dBi and satisfactory performance at different angles of radiation.

The radiation pattern for the PIFA antenna can provide insight into the antenna's recital in terms of gain and radiation directionality. The simulation result of radiation pattern is presented in 3-D form in Fig. 8. This PIFA antenna exhibited an all-out gain of 7.08 dBi at a frequency of 5.5 GHz, with gains of 6.78 dBi at 3.8 GHz, 3.31 dBi at

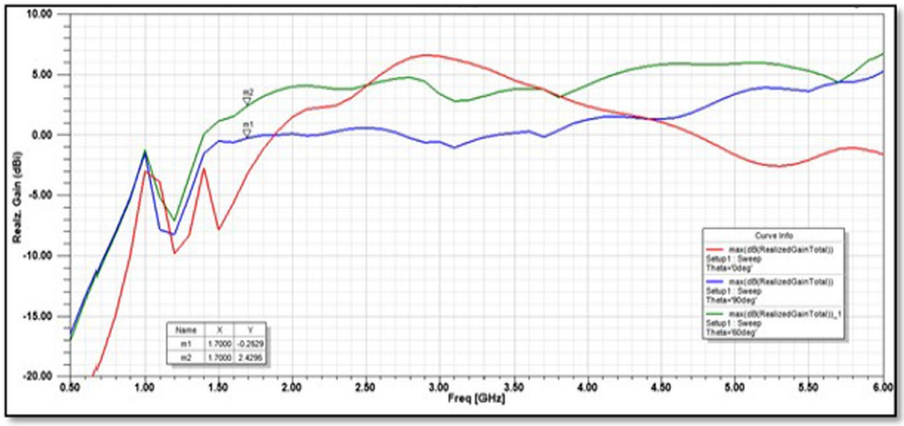

Fig. 7 Max. realized gain over Freq and for Theta 0°, 60° and 90°. The figure shows the maximum realized gain of the antenna over frequency for three different radiation angles: 0°, 60°, and 90°.This is the simulated result of realized gain which indicates that gain has maximum value as the frequency increases. The red marked graph shows realized gain for Theta 0°.The blue marked graph shows realized gain for Theta 60°.The green marked graph shows realized gain for Theta 90. At 0° radiation angle, the antenna has a maximum realized gain of approximately 7.8 dBi at a frequency of 3 GHz, indicating that the antenna is most directive in the broadside direction. At 60° radiation angle, the antenna has a maximum realized gain of approximately 5 dBi at a frequency of 5.8 GHz. At 90° radiation angle, the antenna has a maximum realized gain of approximately 6 dBi at a frequency of 4.50–5.50 GHz

1.7 GHz, 6.81 dBi at 5.2 GHz, and 6.65 dBi at 5.9 GHz. These gains correspond to the maximum radiation intensity in the direction of the main lobe of the antenna's radiation pattern. Without a specific radiation pattern plot, we can assume that the radiation pattern of the PIFA antenna would show a strong steering beam in the direction of the main lobe, where the maximum gain occurs. The shape of the radiation pattern may vary depending on the design of the PIFA antenna, but it should exhibit a relatively narrow beam width in the direction of maximum gain.

Table 2 presents a proportional analysis of the proposed antenna design in this paper with various existing antenna designs described in the works. The evaluation is based on several parameters such as resonating frequencies dimensions, and gain, among others. It highlights the improvements achieved by the proposed antenna design in terms of these parameters.

5 Conclusion

This article introduces a multiband, multifunctional antenna that can operate in a variety of frequency bands, including the LTE/5G/V2X bands from 1 to 5 GHz and the V2X band from 5.850 to 5.925 GHz. The antenna has two cut slots in its wide feeding arm for controlling high-frequency bands and one in its shorting arm for controlling low frequency bands. The S11 parameter and VSWR are tested after the HFSS modeling program has initially predicted the antenna's performance. The findings show that the antenna's maximum gain for 5G frequencies is 7.08 dBi and its minimum VSWR is 2, while its maximum gain for V2X frequencies is 6.65 dBi. The proposed antenna design is, in general, a good fit for multiband antenna applications in automobiles. By grounding the short arm through a 6H and an 11H inductor, it is possible to improve the antenna's performance in low-frequency bands, which is the main target of future study.

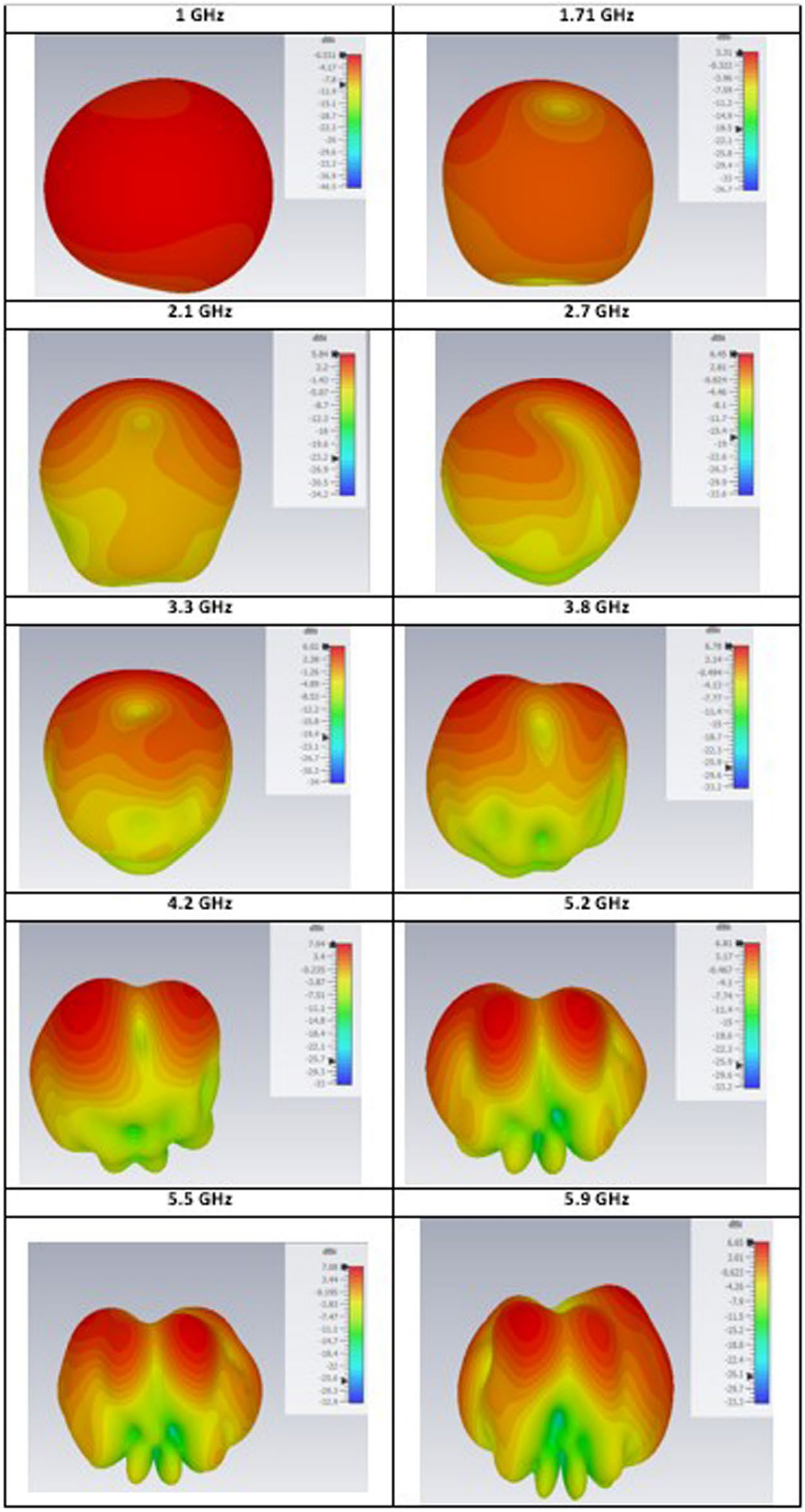

Fig. 8 Radiation pattern realized gain in dBi. The figure shows the 3-D plot of radiation pattern. The radiation pattern realized gain in dBi is a metric used to quantify the directivity of an antenna and is expressed in decibels relative to an isotropic radiator. This PIFA antenna exhibited an all-out gain of 7.08 dBi at a frequency of 5.5 GHz, with gains of 6.78 dBi at 3.8 GHz, 3.31 dBi at 1.7 GHz, 6.81dBi at 5.2 GHz, and 6.65 dBi at 5.9 GHz

Table 2 Comparison between designed antenna and literature

Sr. No	Antenna size $L \times W \times H$ (mm^3)	Substrate	Resonant frequencies (G HZ)	Frequencies range (GHz)	S11 Parameter (db)	Mas gain (db)
[18]	55 × 50 × 28	FR4	1.9/3.6/5	0.617–6	S11 < − 10 db	− 2.1 dBi@617 MHz, − l dBi @ 1.9 GHz, 0 dBi @3.6 GHz and 0.9 dBi @5 GHz
[26]	87 × 1.6 × 60	FR4	–	0.69–0.96 1.7–2.7/(2.4/5)/ DSRC (5.9)	S11 < − 10 db	Gain at 2.4 GHz varies from − 10 to 2.4 dBi Average gain @ 0.69 GHz − 1 dBi/0.96 GHz − 3 dBi/1.7 GHz − 2 dBi/2.7 GHz− 5 dBi Max gain at 5.9 GHz is 2 dBi to the front and − 0.5 dBi to the back
[14]	315 × 30 × 1.6	FR4	2.5/3.5/5.6	2.38–2.92/3.16–4.10	S11 < − 10 db	3.8 dbi/3.2 dbi/5 dbi
[27]	40 × 33 × 0.8	FR4	2.3/3.53/5.5	2.23–2.39/3.41–3.59/	–	1.61 dbi/3.39 dbi/1.78 dbi
[28]	65 × 38.5 × 0.8	FK4	0.95/1.5/2.4	–	–	1.2 dbi/1.2 dbi/1.3 dbi
[29]	60 × 60 × 1.56	FR4	2.6/4.2/4.6	2.31–2.89/ 4.15–4.27/	− 10.28	4.4 dbi/3.9 dbi/3.8 dbi
[30]	50 × 40 × 1.6	FR4	2.4/5/5.87	1.51–3.69/ 4.67–5.25/ 5.78–5.96	− 22.3793 − 18.4588 − 24.8515	5.2 dbi/4.8 dbi/5 dbi
Proposed antenna	54 × 38 × 25	FR4	1.19/2.18/3.5/4.9/5.5/5.9	1.15–1.2/1.58–6	− 12.84/− 29.13 /− 15.93	Max gain obtained 7.08 dbi at frq 5.5 GHz, Gain 6.78 dbi@3.8Ghz , 3.31 dbi@ 1.7 GHz, 6.81 dbi@5 2 GHz, 6.65 dbi@5.9 GHz

Abbreviations

LTE	Long term evolution
V-2-X	Vehicle to everything
PIFA	Planar inverted-F antenna
VSWR	Voltage standing wave ratio
ε	Permittivity
L	Length of substrate
W	Width of substrate
H	Height of antenna
S_g	Gap between the slots
S_l	Length of slot
H_{cut1}, H_{cut2}	Feeding arm cut along height
F_l	Length of feeding
F_h	Height of feeding
W_s	Width of short arm

Acknowledgements
The authors express their gratitude to the Yashwantrao Chavan College of Engineering, Nagpur, India, for providing the testing facility

Author contributions
The antenna was designed, fabricated, and tested by AAN. She also arranged and simulated the necessary models for evaluating the antenna's performance. Both authors have reviewed and approved the final manuscript.

Funding
The authors affirm that no state, national, or international agency, institute, or industry has provided them with a grant or financing for this study project.

Availability of data and materials
Due to the nature of the research, the datasets created and/or analyzed for the current study are not generally accessible, but they are available upon reasonable request from the corresponding author.

Declarations

Competing interests
The authors declare that they have no competing interests.

Received: 11 May 2023 Accepted: 7 September 2023
Published online: 10 October 2023

References
1. K. Abboud, H.A. Omar, W. Zhuang, Interworking of DSRC and cellular network technologies for V2X communications: a survey. IEEE Trans. Veh. Technol. **65**(12), 9457–9470 (2016)
2. E. Ghafari, A. Fuchs, D. Eblenkamp, D.N. Aloi, A vehicular rooftop, shark-fin, multiband antenna for the GPS/LTE/cellular/DSRC systems, in 2014 IEEE-APS Topical Conference on Antennas and Propagation in Wireless Communications (APWC), 237–240, Palm Beach (2014)
3. https://www.its.dot.gov/researcharchives/connectedvehicle/pdf/DSRCReportCongressFINAL23NOV2015.pdf
4. D.V. Navarro Mendez et al., Wideband double monopole for mobile, WLAN and C2C services in vehicular application. IEEE Antennas Wireless Propag. Lett. **16**, 16–19 (2017)
5. D. Garrido Lopez, M. Ignatenko, D.S. Filipovic, Low-profile tri-band inverted-F antenna for vehicular applications in HF and VHF bands. IEEE Trans. Antennas Propag. **63**(11), 4632–4639 (2015)
6. S. Arianos, G. Dassano, F. Vipiana, M. Orefice, Design of multi-frequency compact antennas for automotive communications. IEEE Trans. Antennas Propag. **60**(12), 5604–5612 (2012)
7. G. Artner, W. Kotterman, G. Del Galdo, M.A. Hein, Automotive antenna roof for cooperative connected driving. IEEE Access **7**, 20083–20090 (2019)
8. A. Narbudowicz, X.L. Bao, M.J. Ammann, Dual-band omnidirectional circularly polarized antenna. IEEE Trans. Antennas Propag. **61**(1), 77–83 (2013)
9. G. Fikioris, C. Valagiannopoulos, Input admittances arising from explicit solutions to integral equations for infinite-length dipole antennas. Progr. Electromagn. Res. Lett. **55**, 285–306 (2005)
10. L. Chen, X. Ren, Y.-Z. Yin, Z. Wang, Broadband CPW-fed circularly polarized antenna with an irregular slot for 2.45 GHz RFID reader. Progr. Electromagn. Res. Lett. **41**, 77–86 (2013)
11. C. Valagiannopoulos, An overview of the Watson transformation presented through a simple example. Progr. Electromagn. Res. **75**, 137–152 (2007)
12. K. Sayidmarie, L. Yahya, Modeling of dual-band crescent-shape monopole antenna for WLAN applications. Int. J. Electromagn. Appl. **4**, 31–39 (2014). https://doi.org/10.5923/j.ijea.20140402.01
13. A.M. Franchina, P. Nepa, R. Parolari, I. Moro, A. Polo Filisan, D. Zamberlan, A 3D LTE antenna for vehicular applications, in IEEE International symposium on antennas and propagation & USNC/URSI National Radio Science Meeting, 637–638, San Diego, CA (2017)
14. S. Hasturkoglu, S. Lindenmeier, A wideband automotive antenna for actual and future mobile communication 5G/LTE/WLAN with low profile, in 11th European conference on antennas and propagation (EUCAP), 602–605, Paris (2017)
15. E. Ghafari, D.N. Aloi, Top-loaded UWB monopole antenna for automotive applications, in Proceedings of the 2012 IEEE International Symposium on Antennas and Propagation, 1–2, Chicago, IL (2012)
16. A. Michel, P. Nepa, M. Gallo, I. Moro, A.P. Filisan, D. Zamberlan, Printed wideband antenna for LTE-band automotive applications. IEEE Antennas Wireless Propag. Lett. **16**, 1245–1248 (2017). https://doi.org/10.1109/LAWP.2016.2629619
17. S.S. Bharadwaj et al., A compact tri-band frequency reconfigurable antenna for LTE/Wi-Fi/ITS applications. Progr. Electromagn. Res. M **91**, 59–67 (2020)
18. Y. Cheng, L. Jing, C. Wang, Design of a multiple band vehicle-mounted antenna. Int. J. Antennas Propag. (2019). https://doi.org/10.1155/2019/6098014
19. B.T.P. Madhav, T. Anilkumar, Design and study of multiband planar wheel-like fractal antenna for vehicular communication applications. Microw. Opt. Technol. Lett. **60**(8), 1985–1993 (2018). https://doi.org/10.1002/mop.31290
20. A.S. Ibrahim, A.M. Yacoub, D.N. Aloi, A 3-dimensionalmultiband antenna for vehicular 5G Sub-6 GHz/ GNSS/V2X applications. Int. J. Antennas Propag. (2022). https://doi.org/10.1155/2022/5609110
21. E. Guariglia, Harmonic sierpinski gasket and applications. Entropy **20**(9), 714 (2018)
22. C. Puente-Baliarda, J. Romeu, R. Pous, A. Cardama, On the behavior of the Sierpinski multiband fractal antenna. IEEE Antennas Propag. **46**, 517–524 (1998)
23. E. Guariglia, Entropy and fractal antennas. Entropy **18**(3), 1–17 (2016)
24. C.A. Balanis, *Microstrip Antennas, Antenna Theory, Analysis and Design*, 3rd edn. (Wiley, Hoboken, 2010)
25. P.M. Paul, K. Kandasamy, M.S. Sharawi, A tri-band slot antenna loaded with split ring resonators. Microw. Opt. Technol. Lett. **59**(10), 2638–2643 (2017)
26. A. Yacoub, M. Khalifa, D.N. Aloi, Wide bandwidth low profile PIFA antenna for vehicular sub-6 GHz 5G and V2X wireless systems. Progr. Electromagn. Res. C **109**, 257–273 (2021). https://doi.org/10.2528/PIERC21010609
27. Y. Hua, L. Huang, Y. Lu, A compact 3-port multiband antenna for V2X communication. In 2017 IEEE International Symposium on Antennas and Propagation & USNC/URSI National Radio Science Meeting, 639–640, San Diego, CA (2017)
28. X.-Q. Zhang, Y.-C. Jiao, W.-H. Wang, Compact wide tri-band slot antenna for WLAN/WiMAX applications. Electron Lett. **48**(2), 64–65 (2012)
29. S. Verma, P. Kumar, Compact triple-band antenna for WiMAXand WLAN applications. Electron Lett. **50**(7), 484–486 (2014)

30. S. Mulla, S.S. Deshpande, Compact multiband antenna fed with wideband coupled line impedance transformer for improvement of impedance matching. Microw. Opt. Technol. Lett. **59**(9), 2341–2348 (2017)

Publisher's Note

Springer Nature remains neutral with regard to jurisdictional claims in published maps and institutional affiliations.

Amruta A. Nikam earned her bachelor's in electronics and telecommunication from JDIET College of engineering in Yavatmal in 2008, her master's from KITS, Nagpur University in 2012, and she is currently enrolled in the Ph.D. programme at G. H. Raisoni College of Engineering and Management, Pune, which is part of SPPU, Pune. Her areas of interest in study are antenna, electromagnetics, and wave propagation.

Rupali B. Patil RASHTRASANT TUKADOJI MAHARAJ NAGPUR UNIVERSITY awarded Rupali B. Patil a B.E. in electronics engineering in 2000, and Sant Gadge Baba Amravati University awarded her an M.E. in digital electronics in 2004. Visvesvaraya National Institute of Technology (VNIT), Nagpur, India, is where she obtained her Ph.D. At Savitribai Phule Pune University in Pune, Maharashtra, India, she is currently the Dean (Research and Development) and an Assistant Professor in the Department of Electronics and Telecommunication Engineering. Her areas of interest are wireless communication, cognitive radio, and SDR, and she has 20 years of academic experience. She is an ISTE Life Member.